# Effector caspase Dcp-1 and IAP protein Bruce regulate starvation-induced autophagy during *Drosophila melanogaster* oogenesis

Ying-Chen Claire Hou,[1] Suganthi Chittaranjan,[1] Sharon González Barbosa,[2] Kimberly McCall,[2] and Sharon M. Gorski[1]

[1]The Genome Sciences Centre, British Columbia Cancer Research Centre, Vancouver, British Columbia V5Z 1L3, Canada
[2]Department of Biology, Boston University, Boston MA 02215

A complex relationship exists between autophagy and apoptosis, but the regulatory mechanisms underlying their interactions are largely unknown. We conducted a systematic study of *Drosophila melanogaster* cell death–related genes to determine their requirement in the regulation of starvation-induced autophagy. We discovered that six cell death genes—*death caspase-1* (*Dcp-1*), *hid*, *Bruce*, *Buffy*, *debcl*, and *p53*—as well as *Ras–Raf–mitogen activated protein kinase* signaling pathway components had a role in autophagy regulation in *D. melanogaster* cultured cells. During *D. melanogaster* oogenesis, we found that autophagy is induced at two nutrient status checkpoints: germarium and mid-oogenesis. At these two stages, the effector caspase Dcp-1 and the inhibitor of apoptosis protein Bruce function to regulate both autophagy and starvation-induced cell death. Mutations in *Atg1* and *Atg7* resulted in reduced DNA fragmentation in degenerating midstage egg chambers but did not appear to affect nuclear condensation, which indicates that autophagy contributes in part to cell death in the ovary. Our study provides new insights into the molecular mechanisms that coordinately regulate autophagic and apoptotic events in vivo.

## Introduction

Macroautophagy (hereafter referred to as autophagy) is an evolutionarily conserved mechanism for the degradation of long-lived proteins and organelles. During autophagy, cytoplasmic components are sequestered into double membrane structures called autophagosomes, which then fuse with lysosomes to form autolysosomes, where degradation occurs (for review see Klionsky, 2007). Currently, there are 31 autophagy-related (*Atg*) genes in yeast, and 18 Atg proteins are essential for autophagosome formation (Mizushima, 2007). Most yeast *Atg* genes have orthologues in higher eukaryotes and encode proteins required for autophagy induction, autophagosome nucleation, expansion, and completion, and final retrieval of Atg protein complexes from mature autophagosomes (for review see Levine and Yuan, 2005).

Depending on the physiological and pathological conditions, autophagy has been shown to act as a pro-survival or pro-death mechanism in vertebrates (for reviews see Levine and Yuan, 2005; Maiuri et al., 2007). In the case of growth factor withdrawal, starvation, and neurodegeneration, autophagy has been shown to function in cell survival (Boya et al., 2005; Lum et al., 2005; Hara et al., 2006; Komatsu et al., 2006). In contrast, autophagy has been found to act as a cell death mechanism in derived cell lines where caspases or apoptotic regulators are impaired (Shimizu et al., 2004; Yu et al., 2004). The nature and perhaps level of the stress stimulus may also be important in determining whether autophagy promotes cell survival or cell death (Boya et al., 2005; Maiuri et al., 2007; Wang et al., 2008).

Correspondence to Sharon M. Gorski: sgorski@bcgsc.ca

S.N. González Barbosa's present address is Rio Piedras Campus, University of Puerto Rico, San Juan 00931, Puerto Rico.

Abbreviations used in this paper: 3MA, 3-methyladenine; Atg, autophagy-related; Baf, bafilomycin A1; BIR, baculoviral IAP repeat; Dcp-1, death caspase-1; DIAP1, *Drosophila melanogaster* IAP protein-1; dsRNA, double-stranded RNA; fl-Dcp-1, full-length Dcp-1; GLC, germ line clone; IAP, inhibitor of apoptosis; *l(2) mbn*, lethal (2) malignant blood neoplasm; LC3, microtubule associated protein 1 light chain 3B; LTG, LysoTracker green; LTR, LysoTracker red; PI3K, phosphoinositide 3-kinase; QRT-PCR, quantitative RT-PCR; TOR, target of rapamycin; UASp, upstream activating sequence.

The online version of this article contains supplemental material.



The Rockefeller University Press $30.00
J. Cell Biol. Vol. 182 No. 6 1127–1139
www.jcb.org/cgi/doi/10.1083/jcb.200712091

Overlaps between components in apoptosis and autophagic pathways have been described. Upstream signal transducers in apoptotic pathways, including TNF-related apoptosis-inducing ligand (TRAIL), TNF, Fas-associated protein with death domain (FADD), and death-associated protein kinase (DAPK), have been shown to play a role in autophagy regulation (Prins et al., 1998; Inbal et al., 2002; Mills et al., 2004; Thorburn et al., 2005), and two apoptotic inducers, including sphingolipid and ceramide, can activate autophagy in mammalian cells (Ghidoni et al., 1996; Scarlatti et al., 2004). In addition, two recent studies demonstrate physical and functional interactions between components of apoptosis and autophagy. First, the antiapoptosis protein, Bcl-2, suppresses autophagy through a direct interaction with Beclin 1, a protein required for autophagy (Pattingre et al., 2005). Second, Atg5, which is cleaved by calpain, associates with Bcl-$X_L$, leading to cytochrome *c* release and caspase activation (Yousefi et al., 2006). Further examples and discussion of the connections between apoptosis and autophagy can be found in several recent reviews on this topic (Ferraro and Cecconi, 2007; Maiuri et al., 2007; Thorburn, 2008). The current findings indicate that there is a complex relationship between apoptosis and autophagy, but the regulatory mechanisms underlying the crosstalk between the two processes are still largely unknown.

Autophagy is observed in several *Drosophila melanogaster* tissues during development, and thus *D. melanogaster* is useful as a model to study autophagy in the context of a living organism. 14 *D. melanogaster* annotated genes share significant sequence identity with the yeast *Atg* genes, and, overall, eight *D. melanogaster Atg* homologues have already been shown to be required for autophagy function (Scott et al., 2004; Berry and Baehrecke, 2007). In addition, recent studies demonstrated the role of autophagy in *D. melanogaster* physiological cell death. Loss of *Atg* genes, including *Atg1*, *Atg2*, *Atg3*, *Atg6*, *Atg7*, *Atg8*, *Atg12*, and *Atg18*, inhibited proper degradation of salivary glands during development. Overexpression of Atg1 induced premature salivary gland cell death in a caspase-independent manner (Berry and Baehrecke, 2007). In contrast, caspase activity was required for Atg1-mediated apoptotic death in the fat body (Scott et al., 2007). Mutation of *Atg7* resulted in an inhibition of DNA fragmentation in the midgut but led to an increase of DNA fragmentation in the adult *D. melanogaster* brain (Juhasz et al., 2007). Together, these results further suggest that the mechanistic role of autophagy in cell death and the interrelations between autophagy and apoptosis may be tissue and/or context dependent.

The adult *D. melanogaster* ovary contains 15–20 ovarioles comprised of developing egg chambers, which consist of 16 germ line cells (15 nurse cells and 1 oocyte) surrounded by a layer of somatic follicle cells. The germ line cells originate from stem cells that undergo mitosis to form 16-cell cysts in a specialized region called the germarium. In the late stage of oogenesis, the nurse cells support the development of the oocyte by transferring to it their cytoplasmic contents. After this "dumping" event, the nurse cells undergo cell death, and their remnants are engulfed by the surrounding follicle cells (King, 1970; Spradling, 1993). In addition to this late-stage developmental cell death, egg chambers can be induced to die at two earlier stages, during germarium formation (in region 2) and mid-oogenesis, by factors such as nutrient deprivation, chemical insults, and altered hormonal signaling (Drummond-Barbosa and Spradling, 2001; McCall, 2004). In some respects, cell death during *D. melanogaster* oogenesis is similar to the death of *D. melanogaster* larval salivary glands. Both nurse cells and salivary gland cells are large and polyploid, and the entire tissues undergo cell death simultaneously (McCall, 2004). Notably, morphological features of autophagy have been described during mid-oogenesis cell death in a related species, *Drosophila virilis* (Velentzas et al., 2007), which suggests that the cell death process in ovaries and salivary glands share additional similarities.

Previous studies have focused on characterizing the role of autophagy genes in cell death and determining the paradoxical functions of autophagy (pro-survival and pro-death) in various cell lines and organisms. However, a systematic approach that investigates the involvement of cell death genes in starvation-induced autophagy has not been conducted. Here, we present RNAi analyses to determine whether known cell death–related genes in *D. melanogaster* play a role in autophagy regulation in the lethal (2) malignant blood neoplasm (*l(2)mbn*) cell line. We also used *D. melanogaster* genetics to investigate a role for the effector caspase *death caspase-1* (*Dcp-1*) and the inhibitor of apoptosis (IAP) family member *Bruce* in autophagy regulation in vivo during *D. melanogaster* oogenesis. Further, we examine the function of autophagy genes *Atg7* and *Atg1* in starvation-induced germ line cell death in the *D. melanogaster* ovary.

## Results

### The RNAi screening assay identifies known positive and negative regulators of starvation-induced autophagy in *D. melanogaster l(2)mbn* cells

To quantify starvation-induced autophagy, we used a *D. melanogaster* tumorous larval hemocyte cell line, *l(2)mbn* (Ress et al., 2000), and used LysoTracker green (LTG) dye, which has been shown previously to label lysosomes and autolysosomes in *D. melanogaster* (Scott et al., 2004; Klionsky et al., 2007). Flow cytometry was used to acquire LTG fluorescence of individual cells. Under nutrient-full medium conditions, we detected a basal level of LTG labeling in *l(2)mbn* cells (Fig. 1 A). When cells were transferred into amino acid–deprived medium for 2 h, we observed a detectable increase in LTG labeling. After 4 h of amino acid deprivation, a further increase in the percentage of cells with high LTG fluorescence levels ($LTG^{high}$ population) was observed (Fig. 1 A). To confirm that autophagy is indeed up-regulated under nutrient-deprived conditions in *l(2)mbn* cells, we constructed a stable *l(2)mbn* cell line expressing mammalian microtubule-associated protein 1 light chain 3 (LC3)/Atg8 fused to GFP protein, a widely used marker for autophagy (Klionsky et al., 2007). During autophagy, LC3 conjugates to phosphatidylethanolamine, which then inserts into the autophagosomal membrane. Thus, localization of GFP-LC3 changes from a diffuse cytoplasmic pattern to a punctate autophagosomal membrane-bound pattern that can be monitored by microscopy (Mizushima

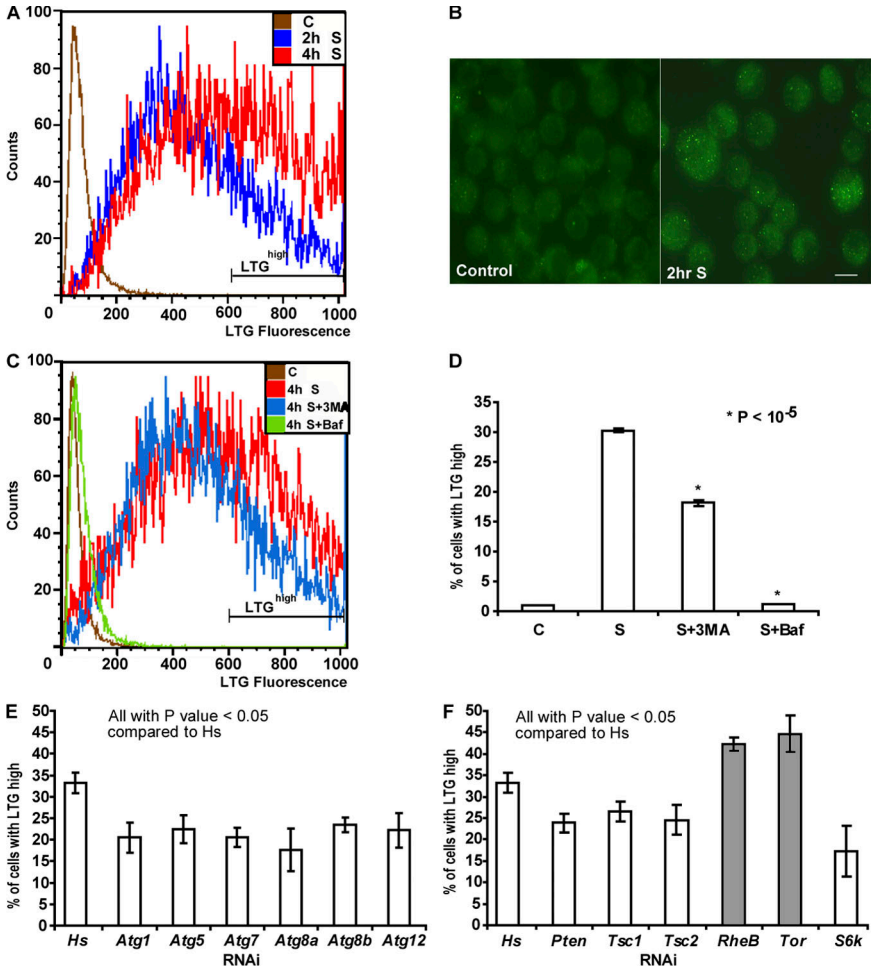


Figure 1. **Quantification of starvation-induced autophagy in *D. melanogaster* l(2)mbn cells.** (A) Flow cytometry analysis of *l(2)mbn* cells starved for 2 h (2h S) or 4 h (4h S) showed an increase in LTG fluorescence levels (x axis) compared with control cells in full-nutrient medium (C). The gate shown on the histogram represents the $LTG^{high}$ population. (B) Representative images of GFP-LC3 puncta in control and 2-h starved *l(2)mbn* cells. An increase in GFP-LC3 puncta was observed in the starved cells (left). Bar, 10 µm. (C) Flow cytometry analysis of 4-h starved cells were incubated with 3MA (4h S + 3MA) and Baf (4h S + Baf). Both autophagy inhibitors reduced the LTG fluorescence levels compared with starved cells (4h S). Control cells in nutrient-full medium (C) are represented by the brown line. (D) Both autophagy inhibitors, 3MA and Baf, reduced the $LTG^{high}$ population significantly. (3MA, P = 0.00001; and Baf, P = 0.00006). (E) RNAi of representative *Atg* genes decreased the LTR fluorescence levels compared with control. (*Atg1*, P = 0.01; *Atg5*, P = 0.01; *Atg7*, P = 0.002; *Atg8a*, P = 0.008; *Atg8b*, P = 0.006; and *Atg12*, P = 0.02). (F) RNAi of all tested genes in the TOR–PI3K pathways had a statistically significant effect on LTG fluorescence levels. Known negative regulators of autophagy are shown with gray bars; positive regulators are shown with white bars. (*Pten*, P = 0.007; *Tsc1*, P = 0.027; *Tsc2*, P = 0.025; *RheB*, P = 0.005; *Tor*, P = 0.016; and *S6k*, P = 0.012). dsRNA corresponding to a human gene (Hs) was used as a negative control in E and F. Results represent the mean value ± SD from at least three independent experiments.

et al., 2001; Klionsky et al., 2007). As expected, the percentage of cells with more than three GFP-LC3 puncta (GFP-LC3 positive) was increased from 9% ($n = 216$) in the nutrient-full condition to 32% ($n = 200$) in the nutrient-starved condition for 2 h (Fig. 1 B). Further, to confirm that LTG labeling correlates with autophagy levels in *l(2)mbn* cells, we used the pharmacological autophagy inhibitors 3-methyladenine (3MA) and bafilomycin A1 (Baf). 3MA blocks autophagy by inhibiting phosphoinositide 3-kinase (PI3K) activity (Seglen and Gordon, 1982). Baf is a specific inhibitor of lysosomal proton pumps and prevents the fusion of autophagosomes with lysosomes (Yamamoto et al., 1998). In *l(2)mbn* cells, both autophagy inhibitors significantly reduced LTG fluorescence levels after starvation treatment (Fig. 1, C and D). Consistently, the addition of 3MA also decreased the numbers of GFP-LC3–positive cells after starvation treatment. As expected, the addition of Baf, which is known to increase the numbers of autophagosomes by preventing their lysosomal degradation, resulted in increased GFP-LC3 puncta in starved cells (Fig. S1 A, available at http://www.jcb.org/cgi/content/full/jcb.200712091/DC1). These results indicate that our flow cytometry–based LTG assay is able to detect changes in the autophagy levels of *l(2)mbn* cells in response to starvation and autophagy-inhibiting drug treatments.

To further validate our flow cytometry–based LTG assay and determine its sensitivity, we used RNAi to specifically inhibit *D. melanogaster* autophagy genes. Currently, there are 14 *D. melanogaster* genes that share significant sequence identity with yeast *Atg* genes, and seven *D. melanogaster Atg* homologues have already been shown to be essential for starvation-induced autophagy in the larval fat body (Scott et al., 2004). In our assay, RNAi of 11 *D. melanogaster Atg* homologues individually resulted in a statistically significant reduction in the $LTG^{high}$ population after starvation treatment (Fig. 1 E and Table S1, available at http://www.jcb.org/cgi/content/full/jcb.200712091/DC1). The effects on LTG staining by RNAi or 3MA were modest in size (e.g., 30–48% change relative to the *Hs*-RNAi–negative control in Fig. 1 E) but reproducible and statistically significant. The limited magnitude of the detectable effects may be due, at least in part, to the nature of this dye as an acidophilic probe that detects autolysosomes but also background lysosomal staining. As with any RNAi-based screen, incomplete target knockdown may also be a contributing factor. Comparison of our RNAi-mediated results with previous in vivo results from the *D. melanogaster* larval fat body (Table S1) indicates that *l(2)mbn* cells require the same autophagy genes as the fat body (Scott et al., 2004).

In higher eukaryotes, starvation-induced autophagy is suppressed by components of the insulin/class I PI3K and target of rapamycin (TOR) pathways (for reviews see Levine and Yuan, 2005; Klionsky, 2007; Maiuri et al., 2007). To determine whether PI3K and TOR pathways are required for starvation-induced

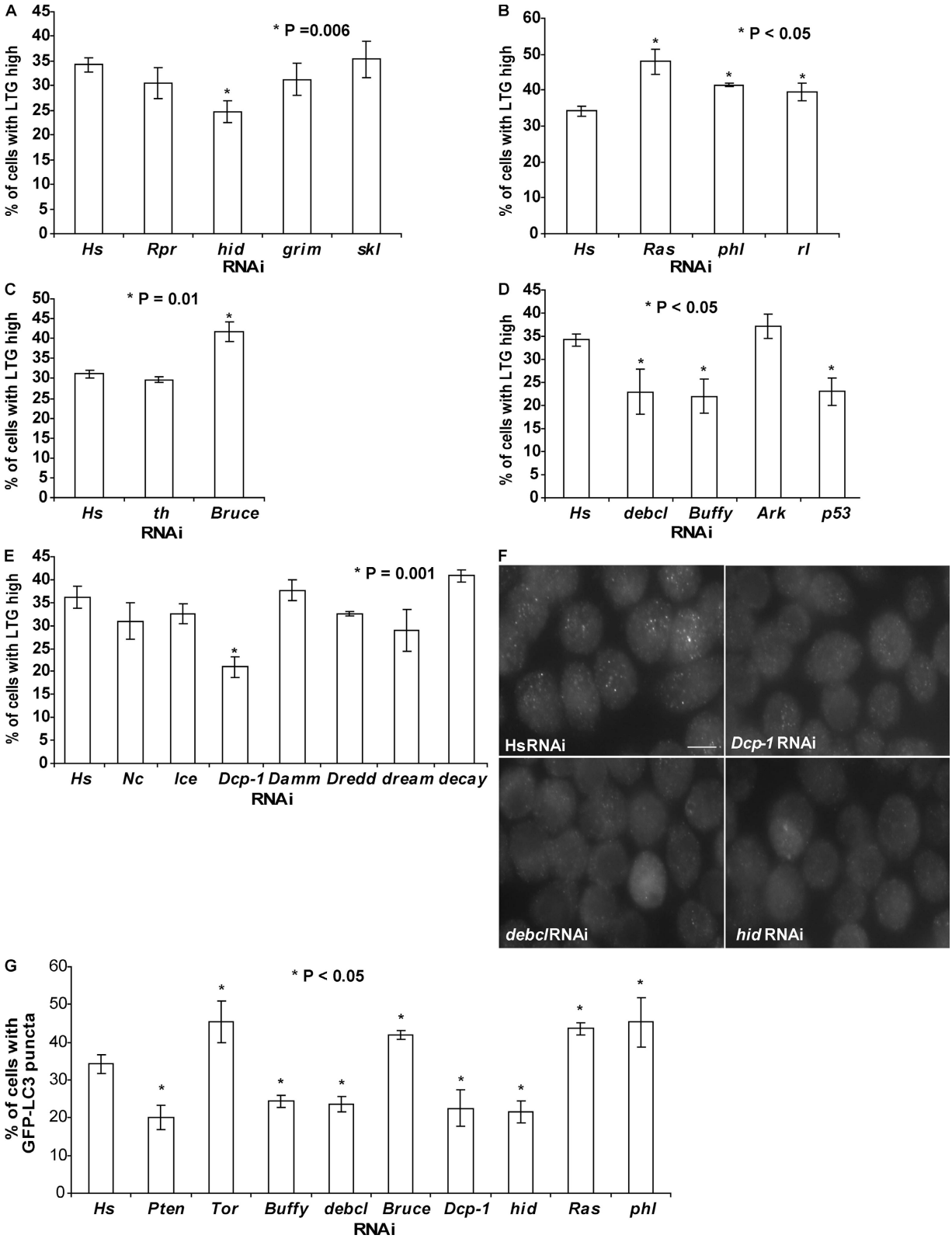


Figure 2. **Identification of known cell death–related genes in autophagy regulation in *l(2)mbn* cells using RNAi.** (A) The percentage of LTG$^{high}$ cells was reduced by *hid*-RNAi (P = 0.006) but not by *rpr*, *grim*, and *skl*-RNAi. (B) Knockdown of *Ras*, *phl*, and *rl* expression by RNAi resulted in an increase in the percentage of LTG$^{high}$ cells. (*Ras*, P = 0.003; *phl*, P = 0.001; and *rl*, P = 0.028). (C) *th*-RNAi treatment (24 h) had no significant effect on LTG levels; in contrast, RNAi of *Bruce* resulted in an increase in LTG fluorescence levels (P = 0.01). (D) Reduction of *debcl*, *Buffy*, or *p53* expression by RNAi resulted in a decrease in LTG fluorescence levels. (*debcl*, P = 0.018; *Buffy*, P = 0.006; and *p53*, P = 0.004). (E) RNAi of effector caspase *Dcp-1* resulted in a significant decrease in the LTG$^{high}$ population (P = 0.001). (F) Representative images of GFP-LC3 puncta in cells treated with the indicated RNAi after a 2-h starvation treatment. Bar, 10 µm. (G) Quantification of cells with GFP-LC3 puncta after RNAi treatment. Cells with more than three GFP-LC3 punctate dots were considered to be GFP-LC3–positive cells. Cells treated with the RNAi indicated here all showed a significant difference (P < 0.05) in the percentage of GFP-LC3–positive

autophagy in *l(2)mbn* cells, we designed double-stranded RNAs (dsRNAs) against several genes in these pathways. RNAi of *Tor* or *RheB*, negative regulators of autophagy, showed an increase in $LTG^{high}$ cells compared with *Hs*-dsRNA (negative control)-treated cells after starvation treatment (Fig. 1 F). In contrast, RNAi of *Pten*, *Tsc1*, *Tsc2*, and *S6k*, positive regulators of autophagy, showed a reduction in the $LTG^{high}$ population (Fig. 1 F). These results indicate that components of TOR and PI3K pathway are essential to regulate starvation-induced autophagy in *D. melanogaster l(2)mbn* cells. These results also demonstrate that our primary screening method, a flow cytometry–based LTG assay, is capable of detecting alterations induced by RNAi-mediated knockdown of positive and negative regulators of autophagy. Thus, this method can be used to identify novel components in starvation-induced autophagy. To ensure that the changes in LTG fluorescence levels were caused by alterations in autophagy, we used GFP-LC3 to track changes in autophagosome formation in cells. RNAi of *Tor* showed an increase in the numbers of GFP-LC3 positive cells after starvation treatment (Fig. 2 G). In contrast, reduction of *Pten* expression by RNAi resulted in a decrease in the number of the GFP-LC3–positive cells (Fig. 2 G). Together, these two methods allow us to monitor the dynamic steps, formation of autophagosomes (GFP-LC3), and autophagosome-lysosome fusion (LTG), during autophagy.

### Identification of cell death–related genes that regulate starvation-induced autophagy in *l(2)mbn* cells

To better understand the relationship between autophagy and apoptosis, we investigated whether known cell death genes were required for starvation-induced autophagy in *l(2)mbn* cells. dsRNAs were designed against the *D. melanogaster* core cell death effectors, *rpr*, *hid*, *grim* and *skl*, and autophagy was evaluated by our flow cytometry–based LTG assay. Only dsRNA corresponding to *hid* but not *rpr*, *grim*, or *skl* showed an effect on autophagy by this assay. RNAi of *hid* decreased the percentage of $LTG^{high}$ cells after starvation treatment (Fig. 2 A). Previous studies showed that the Ras–Raf–MAPK pathway specifically inhibits the proapoptotic activity of *hid* (Bergmann et al., 1998). To determine whether the Ras–Raf–MAPK pathway also plays a regulatory role in autophagy in *l(2)mbn* cells, we designed dsRNAs to target these three components. RNAi of *Ras*, *phl* (also known as *raf*), or *rl* (also known as *MAPK*) all further enhanced the LTG fluorescence levels, suggesting that, like in apoptosis, they have an inhibitory role in autophagy regulation (Fig. 2 B). A second set of dsRNAs, nonoverlapping with the first set of dsRNAs, was designed to validate these new findings, and consistent results were observed (Fig. S1 B). In addition, GFP-LC3 was used to track changes in autophagosome formation in cells. RNAi of *hid* showed a decrease in the numbers of cells with GFP-LC3 puncta (Fig. 2, F and G), whereas RNAi of *Ras*, *phl*, or *rl* all resulted in a significant increase in the numbers of GFP-LC3–positive cells after starvation treatment (Fig. 2 G).

All RHG family members, Rpr, Hid, Grim, and Skl, bind to *D. melanogaster* IAP-1 (DIAP1) and inhibit its antiapoptotic activities (Hay et al., 2004). To test whether DIAP1 (encoded by *th*) is a putative downstream mediator of Hid-dependent autophagy in *l(2)mbn* cells, dsRNA was designed specifically to target *th.* We found that *th*-dsRNA–treated cells showed no difference in LTG fluorescence levels compared with *Hs*-dsRNA (negative control)-treated cells (Fig. 2 C). Interestingly, our data showed that reduced expression of *Bruce*, another IAP family member protein, further increased the LTG fluorescence levels after starvation treatment (confirmed using nonoverlapping dsRNAs; Fig. 2 C; see Fig. S1 C). RNAi of *Bruce* expression also resulted in an increase in GFP-LC3 puncta after starvation treatment (Fig. 2 G). These results suggest that Bruce, instead of DIAP1, could be the downstream target of Hid during starvation induced autophagy in *l(2)mbn* cells.

Next, we investigated whether the transducers of apoptotic signals, *Ark*, *Buffy*, and *debcl*, are required for starvation-induced autophagy. Reduced expression of *Ark*, the *D. melanogaster* homologue of mammalian *Apaf-1*, did not affect the LTG fluorescence levels (Fig. 2 D). RNAi of two Bcl-2 family members, *Buffy* or *debcl*, resulted in a decrease in the percentage of $LTG^{high}$ cells after starvation treatment (Fig. 2 D). Consistently, reduction of *Buffy* and *debcl* expression by RNAi decreased the percentage of GFP-LC3–positive cells after starvation treatment (Fig. 2, F and G). Reduced expression of *Ark*, *Buffy*, and *debcl* was determined using quantitative RT-PCR (QRT-PCR; Fig. S1 D). In addition, we reduced expression of the tumor suppressor *p53* by RNAi and found that starvation-induced autophagy was inhibited (Fig. 2 D). Results were further confirmed using nonoverlapping dsRNAs (Fig. S1 C).

To investigate the requirement of caspases, the final effectors of apoptosis, in starvation-induced autophagy, we designed gene-specific dsRNAs corresponding to seven different *D. melanogaster* caspases. RNAi of just one caspase, *Dcp-1*, but not others resulted in a decrease in the percentage of $LTG^{high}$ cells after starvation treatment (Fig. 2 E). A second dsRNA against *Dcp-1*, nonoverlapping with the first dsRNA, yielded a similar result (Fig. S1 C). Reduction of *Dcp-1* expression by RNAi was determined using QRT-PCR (Fig. S1 D). Consistent with the LTG derived data, RNAi-mediated knockdown of *Dcp-1* resulted in a decrease in GFP-LC3–positive cells after starvation treatment (Fig. 2, F and G). These results indicate that *Dcp-1* functions as a positive regulator of autophagy in *D. melanogaster l(2)mbn* cells.

### Autophagy occurs in response to nutrient deprivation in germaria and midstage egg chambers in the *D. melanogaster* ovary

To further characterize the requirement of Dcp-1 and Bruce in autophagy regulation, we studied *D. melanogaster* oogenesis in vivo. We used a transgenic fly line that expresses a GFP-LC3 fusion protein under the control of the upstream activating

cells compared with the human (Hs) RNAi control. (*Pten*, P = 0.006; *Tor*, P = 0.034; *Buffy*, P = 0.005; debcl, P = 0.003; *Bruce*, P = 0.003; *Dcp-1*, P = 0.007; *hid*, P = 0.002; *Ras*, P = 0.006; and *phl*, P = 0.050). Results represent the mean value ± SD from three independent experiments.

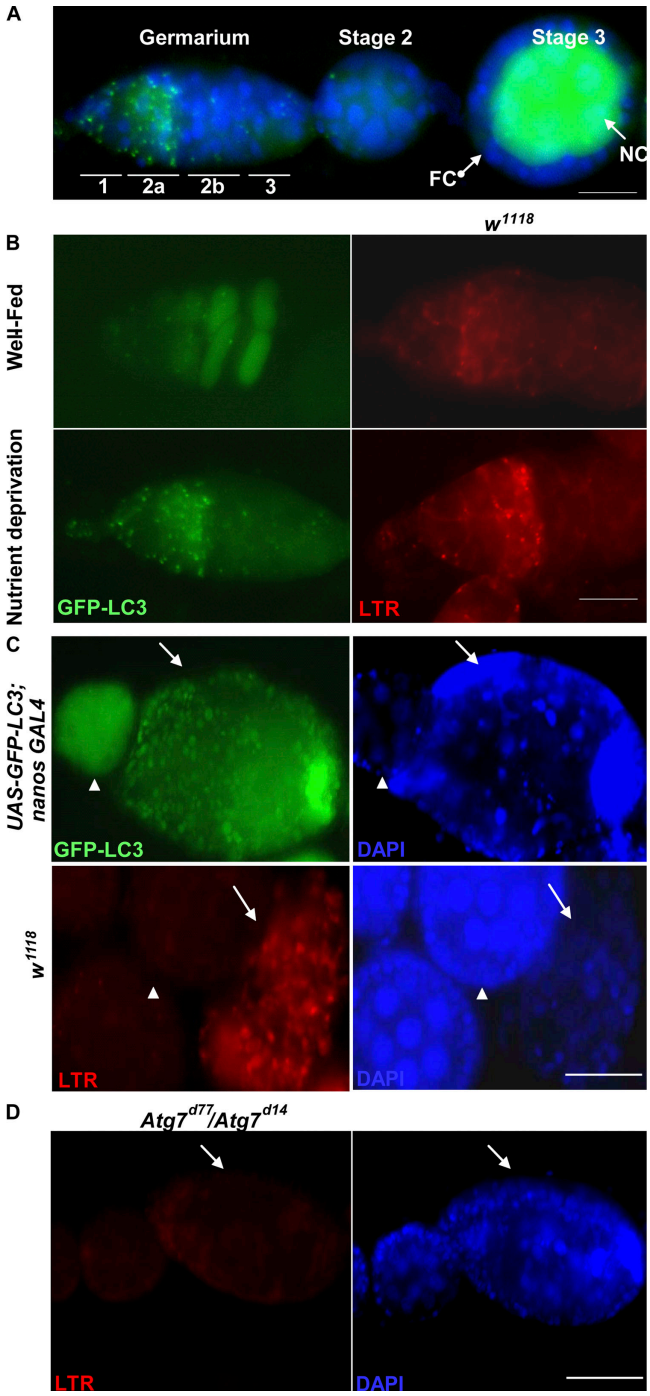


Figure 3. **Nutrient deprivation induces autophagy at region 2 within the germarium and in dying midstage egg chambers.** (A) GFP-LC3 proteins were expressed in nurse cells (NC) but not in follicle cells (FC) by using the *UASp/nanos Gal4* system. DAPI staining of nuclei is shown in blue. (B) *UASp-GFP-LC3; nanos GAL4* flies were conditioned on yeast paste and had a diffuse GFP-LC3 pattern. Numerous GFP-LC3 puncta (green) at region 2 within germarium were observed in nutrient-deprived flies. Ovaries were stained with LTR in $w^{1118}$ flies. Germarium of nutrient-deprived $w^{1118}$ flies had an increase in punctate LTR staining (red) compared with well-fed germarium. (C) Degenerating stage 8 egg chambers (arrows) had numerous GFP-LC3 puncta (green) and an increase in LTR-positive dots (red) compared with healthy egg chambers (arrowheads). DAPI (blue) staining of nuclei is shown in the two panels on the right. (D) Degenerating stage 8 egg chambers (arrows) of nutrient-deprived *Atg7* mutants ($Atg7^{d77}/Atg7^{d14}$) showed a dramatic decrease in LTR staining. DAPI staining of nuclei is shown in blue. Bars: (A and B) 20 µm; (C and D) 50 µm.

sequence (*UASp*) promoter (Rusten et al., 2004). Coexpression of *UASp-GFP-LC3* with the germ line–specific *nanos-GAL4* driver resulted in detectable GFP-LC3 expression in the germ line (nurse cells and oocyte) cells but not in somatic (follicle) cells (Fig. 3 A; Rorth, 1998; Rusten et al., 2004). When *UASp-GFP-LC3; nanos-GAL4 flies* were subjected to nutrient deprivation, we observed numerous GFP-LC3 puncta in region 2 within the germarium (Fig. 3 B). In contrast, flies raised in the presence of yeast paste (Fig. 3 B, well-fed) had a diffuse GFP-LC3 pattern (Fig. 3 B). In addition, we found an increase in punctate LysoTracker red (LTR) staining in germaria of nutrient-deprived wild-type ($w^{1118}$) flies compared with well-fed wild-type flies (Fig. 3 B and Table I). We also observed numerous GFP-LC3 puncta in nutrient-deprived degenerating stage 8 chambers, but a diffuse GFP-LC3 pattern was detected in healthy egg chambers (Fig. 3 C). Similarly, degenerating stage 8 egg chambers had numerous LTR-positive dots in the nurse cells, whereas healthy egg chambers had a low level of LTR staining (Fig. 3 C and Table II). In starved *Atg7* mutants ($Atg7^{d77}/Atg7^{d14}$), there was a significant decrease in punctate LTR staining in region 2 of the germarium and in stage 8 degenerating egg chambers compared with flies with the genotype $CG5335^{d30}/Atg7^{d14}$, which were used previously as controls in Juhasz et al. (2007; Fig. 3 D and Tables I and II). These results indicated that nurse cells lacking the core autophagy regulator *Atg7* failed to induce autophagy in response to nutrient deprivation. Overall, our observations showed that nutrient deprivation induces autophagy in region 2 germaria and in degenerating stage 8 egg chambers in *D. melanogaster*.

## Dcp-1 and Bruce regulate autophagy in germaria and degenerating midstage egg chambers

To determine whether Dcp-1 is required for autophagy at these two specific stages during oogenesis, we used the LTR staining in nutrient-deprived $Dcp\text{-}1^{Prev}$ mutant flies. We observed a decrease in punctate LTR staining in region 2 of the germarium and in stage 8 degenerating egg chambers (Fig. 4, A and B; and Tables I and II) compared with nutrient-deprived wild-type flies. Consistent results were observed using GFP-LC3. Degenerating stage 8 egg chambers in nutrient-deprived $Dcp\text{-}1^{Prev}$ mutants containing the GFP-LC3 transgene had a diffuse GFP-LC3 pattern instead of punctate GFP-LC3 structures (Fig. 4 C). Together, these results indicate that nurse cells lacking *Dcp-1* function are severely impaired in the ability to induce autophagy in response to starvation.

To determine whether Dcp-1 was also sufficient to induce autophagy in vivo, we generated transgenic flies that express the full-length *Dcp-1* (fl-Dcp-1) under the control of the *UASp* promoter. In the presence of a nutrient-rich food source, degenerating stage 8 egg chambers are observed only rarely in wild-type flies (Drummond-Barbosa and Spradling, 2001). However, under nutrient-rich conditions, we observed an abundance of degenerating stage 8 egg chambers in *nanos-GAL4/UASp-fl-Dcp-1* flies with increased levels of punctate LTR staining (Fig. 4 D and Table II). Further, we expressed an activated form of Dcp-1 (missing the prodomain) and GFP-LC3 in the germ line using the *UASp/nanos-GAL4* system and observed numerous degenerating

Table I. **Quantification of autophagy in region 2 germaria**

| Genotype | Nutritional status | LTR positive | Number | Percentage of autophagy |
|---|---|---|---|---|
| $w^{1118}$ | Fed | 8 | 30 | 27 |
| $w^{1118}$ | Nutrient deprivation | 25 | 36 | 69 |
| $Dcp\text{-}1^{Prev}$ | Nutrient deprivation | 17 | 53 | 32 |
| $Bruce^{E81}$ | Fed | 67 | 116 | 58 |
| $Bruce^{E81}/TM3$ | Fed | 18 | 55 | 33 |
| $Bruce^{E16}$ | Fed | 35 | 63 | 56 |
| $Bruce^{E16}/TM3$ | Fed | 13 | 71 | 18 |
| $Atg7^{d77}/Atg7^{d14}$ | Nutrient deprivation | 14 | 65 | 22 |
| $CG5335^{d30}/Atg7^{d14}$ | Nutrient deprivation | 37 | 68 | 54 |

Numbers in the fourth column refer to the numbers of individual germariums scored in at least seven different animals.

stage 8 egg chambers with GFP-LC3 puncta (Fig. 4 E), which indicates that activity of effector caspase Dcp-1 is sufficient to induce autophagy during mid-oogenesis even under nutrient-rich conditions.

We identified the IAP protein Bruce as a negative regulator of autophagy in *l(2)mbn* cells. We next asked whether Bruce is able to inhibit autophagy during *D. melanogaster* oogenesis. We monitored the LTR staining in ovaries of $Bruce^{E81}$ flies that have a deletion in the baculoviral IAP repeat (BIR) domain, which binds to caspases (Arama et al., 2003). In the presence of a nutrient-rich food source, we observed an increase in punctate LTR staining in region 2 of the germarium in $Bruce^{E81}$ flies compared with controls ($Bruce^{E81}/TM3$; Fig. 5 A and Table I). Similarly, we observed numerous degenerating stage 8 egg chambers with increased levels of punctate LTR staining in $Bruce^{E81}$ flies, resembling overexpression of *Dcp-1* (Fig. 5 B and Table II). In well-fed conditions, we observed no degenerating stage 8 egg chamber in control $Bruce^{E81}/TM3$ flies ($n$ = 187 ovarioles; Table II). Punctate LTR staining was similarly observed in region 2 germaria (Table I) and degenerating stage 8 egg chambers (not depicted) in well-fed $Bruce^{E16}$ flies that have a 10-kb deletion in the 3′ end of the *Bruce* gene sequence (Vernooy et al., 2002). Our results demonstrate that Bruce is normally required to inhibit autophagy under nutrient-rich conditions.

### Dcp-1 and Bruce mutants have altered TUNEL staining in germaria and degenerating midstage egg chambers

Our previous work showed that nutrient-deprived *Dcp-1* mutants ($Dcp\text{-}1^{Prev}$) have defects in mid-oogenesis germ line cell death (Laundrie et al., 2003). To determine whether *Dcp-1* is also required for germ line cell death in region 2 within the germarium, we used the TUNEL assay to detect levels of DNA fragmentation as an indication of cell death. We found that nutrient-deprived *Dcp-1* mutants had decreased levels of TUNEL-positive cells in region 2 within the germarium compared with nutrient-deprived wild-type flies (Fig. 6 A and Table III), which indicates that *Dcp-1* is also required for germarium stage cell death.

We also investigated the role of Bruce in cell death during oogenesis. In well-fed $Bruce^{E81}$ flies, we observed a degenerating ovary phenotype that has been shown previously in ovaries with partial loss of another IAP protein, DIAP1 (Xu et al., 2005). This ovary phenotype may be a consequence of excess cell death. Consistent with this possibility, we observed an increased number of cells with TUNEL-positive staining in region 2 within the germarium compared with controls (Fig. 6 A and Table III). Similar results were obtained with $Bruce^{E16}$ flies (Table III). Numerous TUNEL-positive dots were also observed in degenerating stage 8 egg chambers of $Bruce^{E81}$ well-fed flies (Fig. 6 B). These findings demonstrate that Bruce acts as an inhibitor of cell death in germaria and midstage egg chambers.

### Autophagy contributes to cell death in nutrient-deprived ovaries

To assess the role of autophagy that we observed during the germarium and mid-oogenesis stages, we used the TUNEL assay to detect DNA fragmentation in two *Atg* gene mutants. Most *Atg* gene knockouts in *D. melanogaster* result in pupal or larval

Table II. **Quantification of autophagy in stage 8 degenerating egg chambers**

| Genotype | Nutritional status | LTR positive | Number | Percentage of autophagy |
|---|---|---|---|---|
| $w^{1118}$ | Nutrient deprivation | 29 | 40 | 73 |
| $Dcp\text{-}1^{Prev}$ | Nutrient deprivation | 8 | 54 | 15 |
| $Atg7^{d77}/Atg7^{d14}$ | Nutrient deprivation | 13 | 51 | 25 |
| $CG5335^{d30}/Atg7^{d14}$ | Nutrient deprivation | 7 | 14[a] | 50 |
| *nanos-GAL4/UASp-fl-Dcp-1* | Fed | 62 | 74 | 84 |
| $Bruce^{E81}$ | Fed | 43 | 52 | 83 |
| $Bruce^{E81}/TM3$ | Fed | 0 | 0[b] | N/A |

Numbers in the fourth column refer to the number of individual degenerating stage 8 egg chambers scored in at least seven different animals.

[a]$n$ = 4 animals scored for this genotype.

[b]No degenerating stage 8 egg chambers detected.

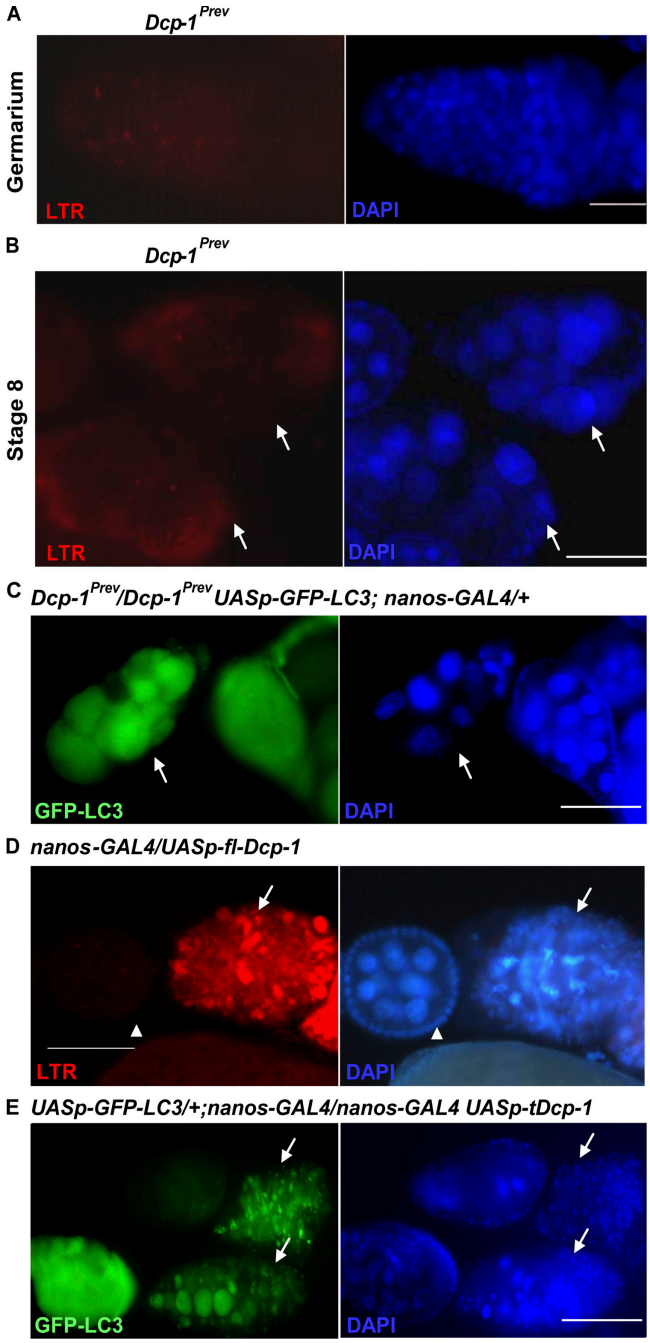


Figure 4. **The effector caspase *Dcp-1* is not only required for nutrient starvation–induced autophagy but is also sufficient for the induction of autophagy during *D. melanogaster* oogenesis.** (A) Germaria of the nutrient-deprived *Dcp-1*$^{Prev}$ flies showed a dramatic decrease in LTR staining compared with nutrient-deprived wild-type flies shown in Fig. 3 B. DAPI staining of nuclei is shown in blue. (B) Degenerating stage 8 egg chambers (arrows) of nutrient-deprived *Dcp-1*$^{Prev}$ flies showed a dramatic decrease in LTR staining compared with nutrient-deprived wild-type flies shown in Fig. 3 C. (C) Lack of Dcp-1 function (*UASp-GFP-LC3 Dcp-1*$^{Prev}$*/Dcp-1*$^{Prev}$*; nanos-GAL4/+*) resulted in uniform diffuse staining of GFP-LC3 rather than the punctate pattern observed in wild-type degenerating stage 8 egg chambers shown in Fig 3 C. (D) Dying egg chambers (arrows) of *NGT/+; nanos-GAL4/UASp-fl-Dcp-1* flies that were conditioned on yeast paste showed a significant increase in punctate LTR staining (red) compared with healthy egg chambers (arrowheads). (E) Expression of activated Dcp-1 (a truncated form) and GFP-LC3 in the germ line (*UASp-GFP-LC3/+; nanos-GAL4/nanos-GAL4 UASp-tDcp-1*) resulted in abundant degenerating stage 8 egg chambers (arrows) with numerous GFP-LC3 puncta (green). DAPI staining of nuclei is shown in blue. Bars: (A) 20 µm; (B–E) 50 µm.

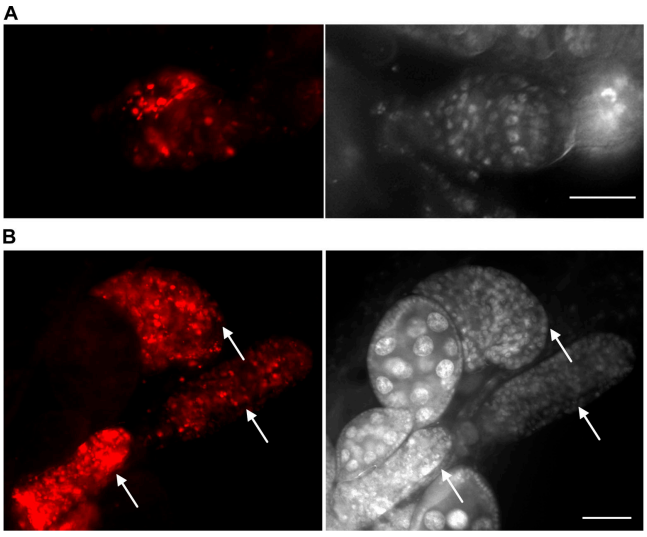


Figure 5. **Bruce suppresses autophagy at region 2 within germarium and in dying stage 8 egg chambers.** (A) The germarium in well-fed *Bruce*$^{E81}$ flies showed an increase in LTR staining (red) compared with wild-type well-fed flies shown in Fig. 3 B (top right). DAPI staining (white) of nuclei is shown on the right. (B) In well-fed wild-type flies, mid-oogenesis nurse cell death is a rare event. Lack of *Bruce* function resulted in an increase in dying stage 8 egg chambers (arrows) in ovaries under well-fed conditions, and these degenerating stage 8 egg chambers had numerous LTR (red) punctate dots. DAPI staining (white) is shown on the right. Bars: (A) 20 µm; (B) 50 µm.

lethality; thus, we first analyzed the fully viable *Atg7* mutant flies (Scott et al., 2004; Juhasz et al., 2007). We found that nutrient-deprived *Atg7* mutants had reduced levels of TUNEL-positive cells in region 2 within the germarium compared with control flies (Table III). Further, degenerating stage 8 egg chambers in starved *Atg7* mutants showed low or no TUNEL-positive staining compared with controls (Fig. 7, A and B; and Table IV). However, nuclear DNA condensation was still observed in the degenerating stage 8 egg chambers of starved *Atg7* mutants (Fig. 7 B). To further investigate the role of autophagy in starvation-induced germ line cell death, we generated *Atg1* germ line clones (GLCs), as mutations in *Atg1* result in lethality at the pupal stage of development (Scott et al., 2004, 2007). Consistent with our *Atg7* mutant observations, nutrient-deprived *Atg1* GLC ovaries had decreased levels of TUNEL staining in both germaria and degenerating stage 8 egg chambers, which indicates a suppression of DNA fragmentation (Fig. 7, C and D; and Tables III and IV). Also consistent with *Atg7*, we observed nuclear DNA condensation in the *Atg1* GLC degenerating stage 8 egg chambers (Fig. 7 D). Our results show that lack of autophagy results in a reduction of DNA fragmentation during starvation-induced cell death in the germaria and midstage egg chambers, which suggests that autophagy contributes to the cell death process at these stages.

## Discussion

Key outstanding questions that need to be addressed are how autophagy and apoptosis pathways interact with each other, and whether common regulatory mechanisms exist between these two processes. We have shown here that six known cell death

Table III. **Quantification of cell death in region 2 germaria**

| Genotype | Nutritional status | TUNEL positive | Number | Percentage of TUNEL |
|---|---|---|---|---|
| $w^{1118}$ | Fed | 9 | 50 | 18 |
| $w^{1118}$ | Nutrient deprivation | 34 | 51 | 67 |
| *Dcp-1*$^{Prev}$ | Nutrient deprivation | 22 | 69 | 32 |
| *Bruce* $^{E81}$ | Fed | 26 | 70 | 37 |
| *Bruce*$^{E81}$*/TM3* | Fed | 12 | 69 | 17 |
| *Bruce*$^{E16}$ | Fed | 20 | 54 | 37 |
| *Bruce*$^{E16}$*/TM3* | Fed | 14 | 80 | 18 |
| *Atg7*$^{d77}$*/Atg7*$^{d14}$ | Nutrient deprivation | 21 | 77 | 27 |
| *CG5335*$^{d30}$*/Atg7*$^{d14}$ | Nutrient deprivation | 95 | 202 | 47 |
| *Atg1* GLC | Nutrient deprivation | 22 | 77 | 29 |
| *Atg1*$^{\Delta 3D}$*/TM3* | Nutrient deprivation | 53 | 64 | 83 |

Numbers in the fourth column refer to the number of individual germariums scored in at least seven different animals.

genes and the Ras–Raf–MAPK signaling pathway not only function in apoptosis but also act to regulate autophagy in *D. melanogaster l(2)mbn* cells. We cannot rule out the possibility that additional cell death genes that we screened may also function in autophagy but were not detected in our assay because of insufficient knockdown by RNAi, a long half-life of the corresponding proteins, and/or functional redundancy.

Consistent with our in vitro data, the involvement of Hid in autophagy regulation has been demonstrated in *D. melanogaster.* Overexpression of Hid induced autophagy in the fat body, larval epidermis, midgut, salivary gland, Malpighian tubules, and trachea epithelium (Juhasz and Sass, 2005). Further, expression of the constitutively active Ras form ($Ras^{V12}$), which has been shown to inhibit Hid activity in apoptosis (Bergmann et al., 1998), can also block Hid-induced autophagy (Juhasz and Sass, 2005). In *D. melanogaster* salivary glands, the Ras signaling pathway has also been shown to inhibit the autophagy process (Berry and Baehrecke, 2007). Based on our loss-of-function findings and these previous gain-of-function studies, we speculate that the Ras–Raf–MAPK pathway acts upstream to inhibit Hid activity in autophagy.

Poor nutrition has a dramatic effect on egg production in *D. melanogaster*. Flies fed on a protein-deprived diet showed an increase in cell death in germaria and midstage egg chambers (Drummond-Barbosa and Spradling, 2001). These two stages have been proposed to serve as nutrient status checkpoints where defective egg chambers are removed before the investment of energy into them. The molecular mechanisms of germarium cell death are still largely unknown, and Daughterless, a helix-loop-helix transcription factor, was the only known regulator involved in cell death of germaria (Smith et al., 2002). Nurse cell death during mid-oogenesis is also different from most developmental cell death in other *D. melanogaster* tissues because apoptotic regulators such as *rpr*, *hid*, or *grim* are not required for cell death in these cells (Peterson et al., 2007). However, the activity of caspases, particularly Dcp-1, was shown to be required for mid-oogenesis cell death (Laundrie et al., 2003; Baum et al., 2007). Our findings implicate several additional genes, *Dcp-1*, *Bruce*, *Atg7*, and *Atg1*, in nutrient deprivation–induced cell death in the germarium, as well as during mid-oogenesis.

Other forms of cell death, such as autophagic cell death, have been proposed previously to be involved in the elimination of defective egg chambers during mid-oogenesis. Known signaling pathways, including the insulin and ecdysone pathways, have been shown to be required not only for the survival of nurse cells in mid-oogenesis; they are also known to regulate the autophagy process, supporting the notion that autophagy plays a role in mid-oogenesis cell death (Drummond-Barbosa and Spradling, 2001; McCall, 2004). Features of autophagy were observed during *D. virilis* mid-oogenesis cell death as shown by monodansylcadaverine staining and transmission electron microscopy (Velentzas et al., 2007). Our results using GFP-LC3 and LTG demonstrate that autophagy occurs in degenerating mid-stage egg chambers and also in germaria of nutrient deprived *D. melanogaster*. We found that mutation of *Atg7* results in a significant decrease of autophagy in dying mid-stage egg chambers and in germaria of starved flies, further supporting the presence of autophagy during these stages.

The role of autophagy in cell survival or cell death is still not well resolved and is likely to be context dependent. Our results show that autophagy contributes to the cell death process in the ovary. Loss of Atg7 or Atg1 activity in both dying mid-stage egg chambers and germaria leads to decreased TUNEL staining, which indicates a reduction in DNA fragmentation.

Table IV. **Quantification of cell death in stage 8 degenerating egg chambers**

| Genotype | Nutritional status | TUNEL positive | Number | Percentage of TUNEL |
|---|---|---|---|---|
| *Atg7*$^{d77}$*/Atg7*$^{d14}$ | Nutrient deprivation | 17 | 69 | 25 |
| *CG5335*$^{d30}$*/Atg7*$^{d14}$ | Nutrient deprivation | 39 | 62 | 63 |
| *Atg1* GLC | Nutrient deprivation | 3 | 16 | 19 |
| *Atg1*$^{\Delta 3D}$*/TM3* | Nutrient deprivation | 19 | 37 | 51 |

Numbers in the fourth column refer to the number of individual degenerating stage 8 egg chambers scored in at least seven different animals.

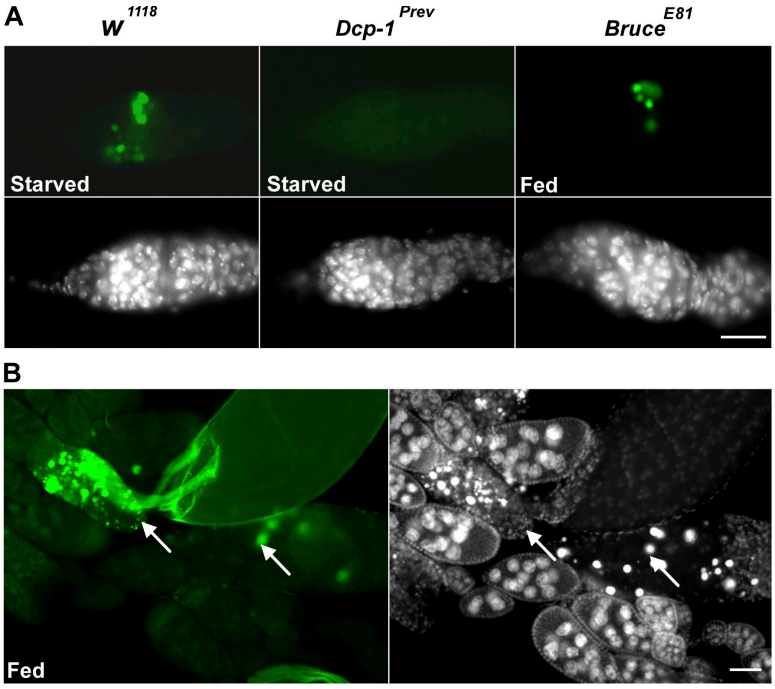


Figure 6. ***Dcp-1* is required for nutrient starvation–induced germarium cell death, and the IAP protein Bruce inhibits germarium and mid-oogenesis cell death.** (A) Ovaries were stained with TUNEL (green) to detect DNA fragmentation. Clusters of cysts with TUNEL staining were observed in region 2 in nutrient-deprived $w^{1118}$ files. In $Dcp\text{-}1^{Prev}$ flies, fewer TUNEL-positive cysts in region 2 were observed. Under well-fed conditions, numerous TUNEL-positive cysts were observed in $Bruce^{E81}$ flies. DAPI staining of nuclei is shown in white. (B) Numerous degenerating stage 8 egg chambers (arrows) with TUNEL-positive staining (green) were observed in well-fed $Bruce^{E81}$ flies. DAPI staining of nuclei (white) is shown on the right. Bars: (A) 20 µm; (B) 50 µm.

Consistent results were observed previously in the larval midguts of *Atg7* mutants, which also showed an inhibition of DNA fragmentation (Juhasz et al., 2007). Interestingly, lack of autophagy function does not appear to affect nuclear DNA condensation in nurse cells. Nurse cells in degenerating stage 8 egg chambers of starved *Atg7* mutants or *Atg1* GLCs appeared to still have condensed nuclei, as shown by DAPI staining (Fig. 7, B and D). Thus, based on *Atg7* and *Atg1* mutant analyses, autophagy contributes to DNA fragmentation but not all aspects of nurse cell death. Future studies are required to determine how autophagy is connected to known pathways leading to DNA fragmentation and chromatin condensation during cell death.

The IAP family member Bruce was shown previously to repress cell death in the *D. melanogaster* eye (Vernooy et al., 2002). Bruce was also shown to protect against excessive nuclear condensation and degeneration, perhaps by limiting excessive caspase activity, during sperm differentiation (Arama et al., 2003). Other IAP family members have been shown to bind caspases via a BIR domain and inhibit apoptosis (Riedl and Shi, 2004). The presence of a BIR domain in Bruce suggests that it may also have caspase-binding activity. We found that lack of Bruce function resulted in an increase in both LTR and TUNEL staining in germaria and degenerating midstage egg chambers. Thus, the *Bruce* mutant-degenerating phenotype in ovaries suggests that Bruce might function normally to restrain or limit caspase activity in this tissue. Because we found that Dcp-1 and Bruce are both required for the regulation of autophagy and DNA fragmentation in germaria and dying midstage egg chambers, it is possible that Bruce acts to bind and degrade Dcp-1 in nurse cells under nutrient-rich conditions. Future studies using epistasis and protein interaction analyses will be required to test this prediction. We cannot rule out the possibility that other IAP proteins, such as DIAP1, and other caspases also play a role during these stages. However, at least in response to starvation signals, Bruce and Dcp-1 play a nonredundant dual role in the regulation of autophagy and cell death in the ovary.

Numerous studies have linked caspase function to apoptosis, but recent findings indicate that caspases are also required for nonapoptotic processes including immunity and cell fate determination (for reviews see Kumar, 2004; Kuranaga and Miura, 2007). We have shown here that Dcp-1 is also required for starvation-induced autophagy. In the ovary, it appears that both apoptotic and autophagic events occur in the germaria and midstage egg chambers after nutrient deprivation. It is possible that Dcp-1 coordinates autophagy and apoptosis at these two nutrient status checkpoints to ensure elimination of defective egg chambers in the most efficient manner possible. *Dcp-1* mutants exhibit intact nuclei in stage 8 defective egg chambers, which indicates a block in both DNA fragmentation and nuclear condensation, and further supports a dual regulatory role for Dcp-1 in mid-oogenesis cell death. Dcp-1 might function to induce autophagosome formation while coordinately acting upon alternate proteolytic targets to complete execution of apoptosis. Future studies to elucidate upstream regulators and downstream substrates of Dcp-1 in cells undergoing autophagy or apoptosis will help to establish the regulatory mechanisms governing the crosstalk between these two cellular processes. Given the multiple cellular effects associated with autophagy, our results also have important therapeutic implications for the use of modulators of caspase or IAP activity in the treatment of cancer and other diseases.

## Materials and methods

### Cell culture conditions

*D. melanogaster l(2)mbn* cells (provided by A. Dorn, Institute of Zoology, Johannes Gutenberg University, Mainz, Germany) were maintained in Schneider's *D. melanogaster* medium (Invitrogen) supplemented with 10% FBS in 25-$cm^2$ suspension flasks (Sarstedt) at 25°C (Ress et al., 2000). All the experiments were performed 3 d after passage and the cells were discarded after 25 passages.

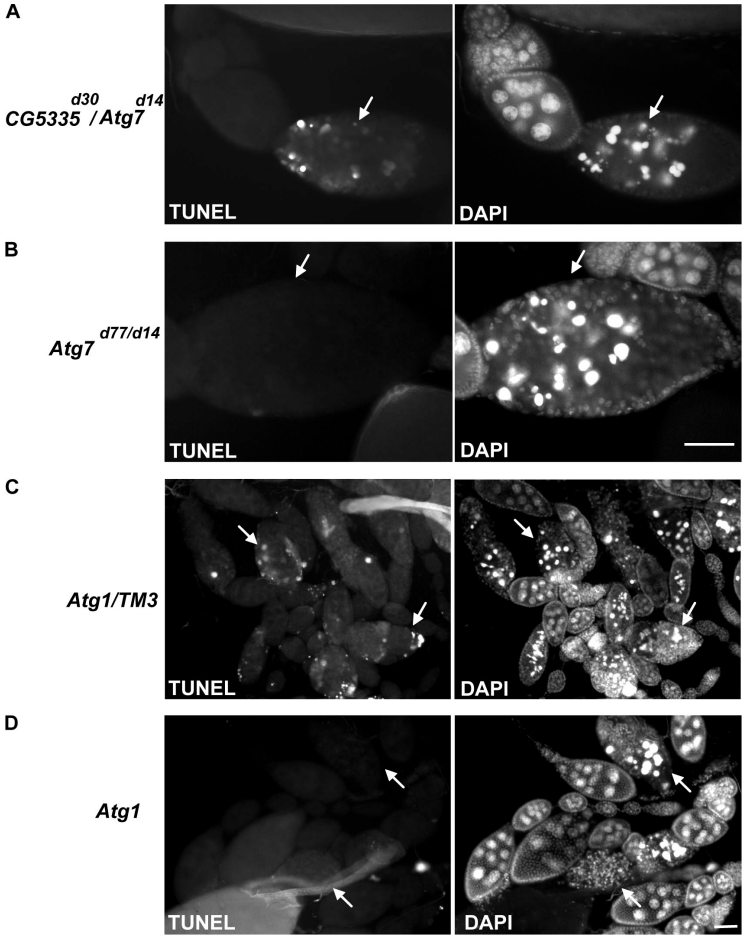


Figure 7. **Lack of Atg7 or Atg1 function reduces DNA fragmentation during mid-oogenesis cell death.** (A) TUNEL-positive staining was observed in dying stage 8 egg chambers (arrows) of starved control flies (*CG5335$^{d30}$/Atg7$^{d14}$*). DAPI staining of nuclei (white) is shown on the right. (B) In nutrient-deprived *Atg7* mutants (*Atg7$^{d77}$/Atg7$^{d14}$*), degenerating stage 8 egg chambers (arrows) showed no or low levels of TUNEL staining. Nuclear DNA condensation, detected by DAPI, was still observed. (C) Dying stage 8 egg chambers (arrows) from nutrient-deprived control siblings (*Atg1$^{\Delta 3D}$/TM3*) generated from the same cross in D had abundant TUNEL-positive staining. (D) In nutrient-deprived *Atg1* GLCs, degenerating stage 8 egg chambers (arrows) showed no or low levels of TUNEL staining. Nuclear DNA condensation (DAPI, right) in degenerating egg chambers appeared to occur as in the controls. Bars, 50 µm.



**dsRNA synthesis**

Individual PCR products containing coding sequences for the transcripts to be targeted were generated by RT-PCR using Superscript one-step RT-PCR kit with platinum taq (Invitrogen). Each primer used in the RT-PCR contained a 5′ T7 RNA polymerase-binding site (TAATACGACTCACTATAGG) followed by sequences specific for the targeted genes (Table S2, available at http://www.jcb.org/cgi/content/full/jcb.200712091/DC1). For in vitro transcription reactions, 50 µl of each of the RT-PCR products was ethanol-precipitated and resuspended in 8 µl of nuclease-free water and then used as template. In vitro transcription reactions were performed using T7 RiboMax Express RNAi systems (Promega) according to the manufacturer's instructions. dsRNAs were ethanol-precipitated and resuspended in 50 µl of nuclease free water. A 5-µl aliquot of 1:100 dilution was analyzed by 1% agarose gel electrophoresis to determine the quality of dsRNA. The dsRNA was quantitated using the PicoGreen assay (Invitrogen) and adjusted to 200 ng/µl with nuclease-free water.

**RNAi**

66 µl of cells ($10^6$ cells/ml) in SFM922 medium were seeded into each well of a 96-well plate. 2 µg of dsRNA (20 µM) was added into each well. After 1 h of incubation at room temperature, the cells received Schneider's medium supplemented with 10% FBS to achieve a final volume of 200 µl. Cells were incubated for 72 h at 25°C.

Because RNAi of *th* triggered a massive amount of apoptosis at the standard incubation time of 72 h, we instead used a 24-h incubation period. After 24 h of *th*-dsRNA treatment, there was already a significant amount of apoptotic cells present, which indicates an efficient knockdown by RNAi, but a sufficient number of healthy cells (>10,000) remained for LTG analysis.

**Flow cytometry–based LTG assay**

For drug treatments, 10 mM 3MA or 0.1 µM Baf was added when nutrient-full medium was replaced with 2 mg/ml glucose in PBS. After a 4-h incubation at 25°C, cells were incubated for 20 min at room temperature with 50 nM LTG for quantification of autophagy levels and 2 µg/ml propidium iodide (PI) to eliminate dead cells. The cells were then analyzed using flow cytometry (FACSCalibur; Becton Dickinson). A minimum of 10,000 cells per sample was acquired for triplicate samples per experiment. LTG fluorescence levels of cells (excluding PI-positive cells) were analyzed using FlowJo software.

For RNAi experiments, the RNAi-treated cells, after a 72-h incubation, were transferred into a U-bottom 96-well plate and centrifuged at 800 rpm for 5 min. Nutrient-full medium was replaced with 2 mg/ml glucose/PBS with 20 µM dsRNA for a 4-h starvation treatment, then cells were labeled with LTG and PI for 20 min at room temperature and finally analyzed as described in the previous section.

**GFP-LC3 detection**

The p2ZOp2F-EGFP-LC3 plasmid was generated by restriction digestion of EGFP-LC3 from pUASP-EGFP-LC3 (Rusten et al., 2004) and cloning into the p2ZOp2F vector (a gift from T. Grigliatti, University of British Columbia, Vancouver, British Columbia, Canada; Hegedus et al., 1998). To create a stable cell line, *D. melanogaster l(2)mbn* cells were transfected with p2ZOp2F-EGFP-LC3 and selected for the presence of the construct using zeocin. The resulting p2ZOp2F-EGFP-LC3 stable (GFP-LC3) *l(2)mbn* cells were maintained in Schneider's *D. melanogaster* medium supplemented with 10% FBS and 10 µg/ml zeocin. 66 µl of these GFP-LC3 *l(2)mbn* cells ($2.5 \times 10^6$ cells/ml) in SFM922 medium were seeded into each well of an 8-well CC2-coated chamber slide (LabTek). Cells were incubated with dsRNAs as described in the previous section, followed by a 4-h starvation treatment. Cells were fixed with 2% paraformaldehyde for 20 min and incubated with anti-GFP antibody (1:200; JL8; Clontech Laboratories, Inc.), followed by anti–mouse immunoglobulin Alexa 488 conjugates (Invitrogen). Cells were mounted with antifade reagent with DAPI at room temperature (SlowFade Gold; Invitrogen). Images were obtained using a 63× objective on a microscope (Axioplan2; all from Carl Zeiss, Inc.) and captured with a cooled mono 12-bit camera (QImaging) and Northern Eclipse image analysis software (Empix Imaging, Inc.). Cells with more than three GFP-LC3 punctate dots were

considered to be GFP-LC3–positive cells. A minimum of 200 cells per sample were counted manually for triplicate samples per experiment.

### Statistical analysis

Two-tailed student's *t* test (equal variances) was used to compare mean levels. $n = 3$. $P < 0.05$ was considered statistically significant.

### Generation of transgenic flies

The *UASp-full-length-Dcp-1* construct was generated by PCR amplification of the coding region from a *Dcp-1* cDNA clone (Song et al., 1997) and cloning into the *UASp* vector (Rorth, 1998). Transgenic flies were generated using standard procedures. To express full-length *Dcp-1* in the germ line, flies were crossed to *NGT; nanosGAL4* flies (Cox and Spradling, 2003), and the resulting progeny were analyzed. To express truncated Dcp-1 and GFP-LC3 in the germ line, *yw; nanosGAL4 UASp-tDcp-1* were crossed to *UASp-GFP-LC3; nanos GAL4*, and the resulting progeny were analyzed (Peterson et al., 2003).

### Fly strains

$w^{1118}$ was used as the wild-type stock. Other fly stocks used were as follows: $Dcp\text{-}1^{Prev1}$ and *UASp-GFP-LC3*; *nanos-GAL4* (from H. Stenmark, Norwegian Radium Hospital, Montebello, Oslo, Norway), $Bruce^{E81}$ (from H. Steller, the Rockefeller University, New York, NY), $Bruce^{E16}$ (from B.A. Hay, California Institute of Technology, Pasadena, CA), $Atg7^{d77}$, $Atg7^{d14}$, $CG5335^{d30}$, *and* $Atg1^{\Delta 3D}$ (from T. Neufeld, University of Minnesota, Minneapolis, MN).

### Generation of *Atg 1* GLCs

To generate germ line clones, *FRT2A* was recombined onto the $Atg1^{\Delta 3D}$ chromosome. Correct recombinants were confirmed by failure to complement $Df(3L)Bsc^{10}$ and $Atg1^{00305}$. Germ line clones were generated with the *FLP/FRT/ovoD* technique as described previously (Chou and Perrimon, 1996). Larvae of the genotype *HSflp; ovoD FRT2A/*$Atg1^{\Delta 3D}$ *FRT2A* were heat-shocked on days 4 and 5 for 1 h at 37°C.

### LTR staining

For nutrient-deprivation experiments, flies were conditioned on yeast paste for 2 d and then placed in a dry vial with access to a 10% sucrose solution for 4–5 d (Peterson et al., 2003).

Ovaries were dissected in PBS and immediately transferred into PBS containing 0.8 µM LTR (Invitrogen) for 5 min at room temperature in the dark. The ovaries were then stained with 0.1 mg/ml DAPI for 30 s. The ovaries were washed three times with PBS and mounted with SlowFade antifade reagent at room temperature. Images were obtained using a 20 or 40× objective (Carl Zeiss, Inc.) on an Axioplan2 microscope and captured with a cooled mono 12-bit camera and Northern Eclipse image analysis software. Egg chambers with >10 LTR positive spots were considered to be LTR positive. Stage 8 degenerating egg chambers in $w^{1118}$ flies were scored by the presence of condensed nurse cell nuclei. The degenerating egg chambers in $Dcp\text{-}1^{Prev}$ files were characterized by a disappearance of follicle cells and a persistence of nurse cell nuclei, as described previously (Laundrie et al., 2003).

For expression of *Dcp-1* in ovaries, *NGT/+; nanos-GAL4/UASp-fl-Dcp-1* flies were conditioned on wet yeast paste for 2–4 d and dissected in Ringers solution (Verheyen and Cooley, 1994). Ovaries were incubated with 50 µM LTR DND-99 in PBS for three minutes, washed three times for 5 min each in PBS, fixed for 10 min in 1:1 heptane/3.7% formaldehyde in Pipes buffer (0.1 M Pipes, 2 mM MgSO4, and 1 mM EGTA, pH 6.9), washed three times for 5 min in PBT (PBS + 0.1% Triton X-100), and mounted in antifade + 1.5 µg/ml Hoechst 33258. Egg chambers were viewed at room temperature using a UPlanFl 20×, 0.50 NA objective (Olympus) on a confocal microscope (BX50; Olympus). Images were captured using a Magnafire SP (S99810; Olympus; Hoechst) and Fluoview (LTR) cameras (Olympus). 1,4-diazabicyclo(2,2,2) octane (DABCO) was used as the imaging medium. Egg chambers with >10 LTR-positive spots were considered to be LTR positive. All figures were processed with Photoshop 7.0 (Adobe). Color was added to the LysoTracker image using ImageJ.

### TUNEL assay

Ovaries were dissected in Schneider's *D. melanogaster* medium supplemented with 10% FBS. The ovaries were fixed in PBS containing 4% paraformaldehyde. The ovaries were then washed two times (5 min each) in PBS and permeabilized with 0.2% Triton X-100 for 5 min, followed by two washes in PBS. The TUNEL reaction was performed with the DeadEnd fluorometric TUNEL system (Promega). The ovaries were then stained with 0.1 mg/ml DAPI for 30 s at room temperature, mounted in SlowFade antifade reagent and observed under an Axioplan 2 microscope. Images were obtained using a 10, 20, or 40× objective (Carl Zeiss, Inc.) on an Axioplan2 microscope and captured with a cooled mono 12-bit camera and Northern Eclipse image analysis software.

### QRT-PCR

Cells ($\sim 2 \times 10^5$ cells in 600 µl) were incubated with dsRNAs as described (see "RNAi") at 25°C for 72 h, followed by a 4-h starvation treatment. Cell cultures were transferred to RNase-free Eppendorf tubes (Ambion), and cells were pelleted at 1,000 rpm for 10 min. Cells were lysed in 1 ml Trizol (Invitrogen), and total RNA was extracted according to manufacturer's instructions. Isolated RNA was treated with RNase-free DNase, and 50 ng of total RNA was used in a 15-µl QRT-PCR reaction. QRT-PCR was performed using the one-step SYBR green RT-PCR reagent kit (Applied Biosystems) on a sequence detection system (7900; Applied Biosystems). Expression levels were calculated using the Comparative $C_T$ method with *D. melanogaster rp49* as the reference. All samples were analyzed in triplicate. The knockdown efficiency was determined by comparing the fold change in expression between target dsRNA treated and untreated cells.

### Online supplemental material

Fig. S1 includes representative images of GFP-LC3 puncta in *l(2)mbn* cells after starvation and treatment with autophagy inhibitors. Quantitative LTG data for additional nonoverlapping dsRNAs is also presented, along with assessment of target knockdown by QRT-PCR for selected genes. Table S1 shows a comparison of essential autophagy genes in the *D. melanogaster* larval fat body and *l(2)mbn* cells. Table S2 contains all primer sequences used for the preparation of dsRNAs. Online supplemental material is available at http://www.jcb.org/cgi/content/full/jcb.200712091/DC1.

We are grateful to A. Dorn for *l(2)mbn* cells, T.E. Rusten and H. Stenmark for the EGFP-LC3 plasmid and the *UASp-GFP-LC3; nanos-GAL4 D. melanogaster* strain, and T. Grigliatti for the p2ZOp2F plasmid. We thank B. Hay, T. Neufeld, and H. Steller for fly stocks. For technical assistance, we thank A.H. Tien, C. Helgason, J. Wilton, D. Mateos San Martin, E. Tanner, J. Chang, and B. Laundrie Stahl. We also thank M. Marra, M. Griffith, J. Halaschek-Wiener, and members of the Gorski laboratory for technical advice and helpful comments.

This work was supported by Canadian Institutes of Health Research grant MOP-78882 to S.M. Gorski. It was also supported by National Institutes of Health grant R01 GM60574 to K. McCall and the Summer Undergraduate Research Fellowship program at Boston University (to S.N. González Barbosa). S.N. González Barbosa was supported by the National Science Foundation–funded Northeast Alliance for Graduate Education and the Professoriate grant (NSF No. 0450339).

Submitted: 17 December 2007
Accepted: 19 August 2008

## References

Arama, E., J. Agapite, and H. Steller. 2003. Caspase activity and a specific cytochrome C are required for sperm differentiation in *Drosophila*. *Dev. Cell.* 4:687–697.

Baum, J.S., E. Arama, H. Steller, and K. McCall. 2007. The *Drosophila* caspases Strica and Dronc function redundantly in programmed cell death during oogenesis. *Cell Death Differ.* 14:1508–1517.

Bergmann, A., J. Agapite, K. McCall, and H. Steller. 1998. The *Drosophila* gene hid is a direct molecular target of Ras-dependent survival signaling. *Cell.* 95:331–341.

Berry, D.L., and E.H. Baehrecke. 2007. Growth arrest and autophagy are required for salivary gland cell degradation in *Drosophila*. *Cell.* 131:1137–1148.

Boya, P., R.A. Gonzalez-Polo, N. Casares, J.L. Perfettini, P. Dessen, N. Larochette, D. Metivier, D. Meley, S. Souquere, T. Yoshimori, et al. 2005. Inhibition of macroautophagy triggers apoptosis. *Mol. Cell. Biol.* 25:1025–1040.

Chou, T.B., and N. Perrimon. 1996. The autosomal FLP-DFS technique for generating germline mosaics in *Drosophila melanogaster*. *Genetics.* 144:1673–1679.

Cox, R.T., and A.C. Spradling. 2003. A Balbiani body and the fusome mediate mitochondrial inheritance during *Drosophila* oogenesis. *Development.* 130:1579–1590.

Drummond-Barbosa, D., and A.C. Spradling. 2001. Stem cells and their progeny respond to nutritional changes during *Drosophila* oogenesis. *Dev. Biol.* 231:265–278.

Ferraro, E., and F. Cecconi. 2007. Autophagic and apoptotic response to stress signals in mammalian cells. *Arch. Biochem. Biophys.* 462:210–219.

Ghidoni, R., J.J. Houri, A. Giuliani, E. Ogier-Denis, E. Parolari, S. Botti, C. Bauvy, and P. Codogno. 1996. The metabolism of sphingo(glyco)lipids is correlated with the differentiation-dependent autophagic pathway in HT-29 cells. *Eur. J. Biochem.* 237:454–459.

Hara, T., K. Nakamura, M. Matsui, A. Yamamoto, Y. Nakahara, R. Suzuki-Migishima, M. Yokoyama, K. Mishima, I. Saito, H. Okano, and N. Mizushima. 2006. Suppression of basal autophagy in neural cells causes neurodegenerative disease in mice. *Nature.* 441:885–889.

Hay, B.A., J.R. Huh, and M. Guo. 2004. The genetics of cell death: approaches, insights and opportunities in *Drosophila*. *Nat. Rev. Genet.* 5:911–922.

Hegedus, D.D., T.A. Pfeifer, J. Hendry, D.A. Theilmann, and T.A. Grigliatti. 1998. A series of broad host range shuttle vectors for constitutive and inducible expression of heterologous proteins in insect cell lines. *Gene.* 207:241–249.

Inbal, B., S. Bialik, I. Sabanay, G. Shani, and A. Kimchi. 2002. DAP kinase and DRP-1 mediate membrane blebbing and the formation of autophagic vesicles during programmed cell death. *J. Cell Biol.* 157:455–468.

Juhasz, G., and M. Sass. 2005. Hid can induce, but is not required for autophagy in polyploid larval *Drosophila* tissues. *Eur. J. Cell Biol.* 84:491–502.

Juhasz, G., B. Erdi, M. Sass, and T.P. Neufeld. 2007. Atg7-dependent autophagy promotes neuronal health, stress tolerance, and longevity but is dispensable for metamorphosis in *Drosophila*. *Genes Dev.* 21:3061–3066.

King, R.C. 1970. Ovarian Development in *Drosophila melanogaster*. Academic Press, New York. 227 pp.

Klionsky, D.J. 2007. Autophagy: from phenomenology to molecular understanding in less than a decade. *Nat. Rev. Mol. Cell Biol.* 8:931–987.

Klionsky, D.J., A.M. Cuervo, and P.O. Seglen. 2007. Methods for monitoring autophagy from yeast to human. *Autophagy.* 3:181–206.

Komatsu, M., S. Waguri, T. Chiba, S. Murata, J. Iwata, I. Tanida, T. Ueno, M. Koike, Y. Uchiyama, E. Kominami, and K. Tanaka. 2006. Loss of autophagy in the central nervous system causes neurodegeneration in mice. *Nature.* 441:880–884.

Kumar, S. 2004. Migrate, differentiate, proliferate, or die: pleiotropic functions of an apical "apoptotic caspase". *Sci. STKE.* 2004:pe49.

Kuranaga, E., and M. Miura. 2007. Nonapoptotic functions of caspases: caspases as regulatory molecules for immunity and cell-fate determination. *Trends Cell Biol.* 17:135–144.

Laundrie, B., J.S. Peterson, J.S. Baum, J.C. Chang, D. Fileppo, S.R. Thompson, and K. McCall. 2003. Germline cell death is inhibited by P-element insertions disrupting the dcp-1/pita nested gene pair in *Drosophila*. *Genetics.* 165:1881–1888.

Levine, B., and J. Yuan. 2005. Autophagy in cell death: an innocent convict? *J. Clin. Invest.* 115:2679–2688.

Lum, J.J., D.E. Bauer, M. Kong, M.H. Harris, C. Li, T. Lindsten, and C.B. Thompson. 2005. Growth factor regulation of autophagy and cell survival in the absence of apoptosis. *Cell.* 120:237–248.

Maiuri, M.C., E. Zalckvar, A. Kimchi, and G. Kroemer. 2007. Self-eating and self-killing: crosstalk between autophagy and apoptosis. *Nat. Rev. Mol. Cell Biol.* 8:741–752.

McCall, K. 2004. Eggs over easy: cell death in the *Drosophila* ovary. *Dev. Biol.* 274:3–14.

Mills, K.R., M. Reginato, J. Debnath, B. Queenan, and J.S. Brugge. 2004. Tumor necrosis factor-related apoptosis-inducing ligand (TRAIL) is required for induction of autophagy during lumen formation in vitro. *Proc. Natl. Acad. Sci. USA.* 101:3438–3443.

Mizushima, N. 2007. Autophagy: process and function. *Genes Dev.* 21:2861–2873.

Mizushima, N., A. Yamamoto, M. Hatano, Y. Kobayashi, Y. Kabeya, K. Suzuki, T. Tokuhisa, Y. Ohsumi, and T. Yoshimori. 2001. Dissection of autophagosome formation using Apg5-deficient mouse embryonic stem cells. *J. Cell Biol.* 152:657–668.

Pattingre, S., A. Tassa, X. Qu, R. Garuti, X.H. Liang, N. Mizushima, M. Packer, M.D. Schneider, and B. Levine. 2005. Bcl-2 antiapoptotic proteins inhibit Beclin 1-dependent autophagy. *Cell.* 122:927–939.

Peterson, J.S., M. Barkett, and K. McCall. 2003. Stage-specific regulation of caspase activity in *Drosophila* oogenesis. *Dev. Biol.* 260:113–123.

Peterson, J.S., B.P. Bass, D. Jue, A. Rodriguez, J.M. Abrams, and K. McCall. 2007. Noncanonical cell death pathways act during *Drosophila* oogenesis. *Genesis.* 45:396–404.

Prins, J.B., E.C. Ledgerwood, P. Ameloot, P. Vandenabeele, P.R. Faraco, N.A. Bright, S. O'Rahilly, and J.R. Bradley. 1998. Tumor necrosis factor-induced cytotoxicity is not related to rates of mitochondrial morphological abnormalities or autophagy-changes that can be mediated by TNFR-I or TNFR-II. *Biosci. Rep.* 18:329–340.

Ress, C., M. Holtmann, U. Maas, J. Sofsky, and A. Dorn. 2000. 20-Hydroxyecdysone-induced differentiation and apoptosis in the *Drosophila* cell line, l(2)mbn. *Tissue Cell.* 32:464–477.

Riedl, S.J., and Y. Shi. 2004. Molecular mechanisms of caspase regulation during apoptosis. *Nat. Rev. Mol. Cell Biol.* 5:897–907.

Rorth, P. 1998. Gal4 in the *Drosophila* female germline. *Mech. Dev.* 78:113–118.

Rusten, T.E., K. Lindmo, G. Juhasz, M. Sass, P.O. Seglen, A. Brech, and H. Stenmark. 2004. Programmed autophagy in the *Drosophila* fat body is induced by ecdysone through regulation of the PI3K pathway. *Dev. Cell.* 7:179–192.

Scarlatti, F., C. Bauvy, A. Ventruti, G. Sala, F. Cluzeaud, A. Vandewalle, R. Ghidoni, and P. Codogno. 2004. Ceramide-mediated macroautophagy involves inhibition of protein kinase B and up-regulation of beclin 1. *J. Biol. Chem.* 279:18384–18391.

Scott, R.C., O. Schuldiner, and T.P. Neufeld. 2004. Role and regulation of starvation-induced autophagy in the *Drosophila* fat body. *Dev. Cell.* 7:167–178.

Scott, R.C., G. Juhasz, and T.P. Neufeld. 2007. Direct induction of autophagy by Atg1 inhibits cell growth and induces apoptotic cell death. *Curr. Biol.* 17:1–11.

Seglen, P.O., and P.B. Gordon. 1982. 3-Methyladenine: specific inhibitor of autophagic/lysosomal protein degradation in isolated rat hepatocytes. *Proc. Natl. Acad. Sci. USA.* 79:1889–1892.

Shimizu, S., T. Kanaseki, N. Mizushima, T. Mizuta, S. Arakawa-Kobayashi, C.B. Thompson, and Y. Tsujimoto. 2004. Role of Bcl-2 family proteins in a non-apoptotic programmed cell death dependent on autophagy genes. *Nat. Cell Biol.* 6:1221–1228.

Smith, J.E. III, C.A. Cummings, and C. Cronmiller. 2002. Daughterless coordinates somatic cell proliferation, differentiation and germline cyst survival during follicle formation in *Drosophila*. *Development.* 129:3255–3267.

Song, Z., K. McCall, and H. Steller. 1997. DCP-1, a *Drosophila* cell death protease essential for development. *Science.* 275:536–540.

Spradling, A.C. 1993. The Development of *Drosophila melanogaster.* Cold Spring Harbor Laboratory Press, Cold Spring Harbor, NY. 1558 pp.

Thorburn, A. 2008. Apoptosis and autophagy: regulatory connections between two supposedly different processes. *Apoptosis.* 13:1–9.

Thorburn, J., F. Moore, A. Rao, W.W. Barclay, L.R. Thomas, K.W. Grant, S.D. Cramer, and A. Thorburn. 2005. Selective inactivation of a Fas-associated death domain protein (FADD)-dependent apoptosis and autophagy pathway in immortal epithelial cells. *Mol. Biol. Cell.* 16:1189–1199.

Velentzas, A.D., I.P. Nezis, D.J. Stravopodis, I.S. Papassideri, and L.H. Margaritis. 2007. Mechanisms of programmed cell death during oogenesis in *Drosophila* virilis. *Cell Tissue Res.* 327:399–414.

Verheyen, E., and L. Cooley. 1994. Looking at oogenesis. *Methods Cell Biol.* 44:545–561.

Vernooy, S.Y., V. Chow, J. Su, K. Verbrugghe, J. Yang, S. Cole, M.R. Olson, and B.A. Hay. 2002. *Drosophila* Bruce can potently suppress Rpr- and Grim-dependent but not Hid-dependent cell death. *Curr. Biol.* 12:1164–1168.

Wang, Y., R. Singh, A.C. Massey, S.S. Kane, S. Kaushik, T. Grant, Y. Xiang, A.M. Cuervo, and M.J. Czaja. 2008. Loss of macroautophagy promotes or prevents fibroblast apoptosis depending on the death stimulus. *J. Biol. Chem.* 283:4766–4777.

Xu, D., Y. Li, M. Arcaro, M. Lackey, and A. Bergmann. 2005. The CARD-carrying caspase Dronc is essential for most, but not all, developmental cell death in *Drosophila*. *Development.* 132:2125–2134.

Yamamoto, A., Y. Tagawa, T. Yoshimori, Y. Moriyama, R. Masaki, and Y. Tashiro. 1998. Bafilomycin A1 prevents maturation of autophagic vacuoles by inhibiting fusion between autophagosomes and lysosomes in rat hepatoma cell line, H-4-II-E cells. *Cell Struct. Funct.* 23:33–42.

Yousefi, S., R. Perozzo, I. Schmid, A. Ziemiecki, T. Schaffner, L. Scapozza, T. Brunner, and H.U. Simon. 2006. Calpain-mediated cleavage of Atg5 switches autophagy to apoptosis. *Nat. Cell Biol.* 8:1124–1132.

Yu, L., A. Alva, H. Su, P. Dutt, E. Freundt, S. Welsh, E.H. Baehrecke, and M.J. Lenardo. 2004. Regulation of an ATG7-beclin 1 program of autophagic cell death by caspase-8. *Science.* 304:1500–1502.